Crystal structures of the apo and ATP bound *Mycobacterium tuberculosis* nitrogen regulatory PII protein

Nishant D. Shetty,[1] Manchi C. M. Reddy,[2] Satheesh K. Palaninathan,[2] Joshua L. Owen,[2] and James C. Sacchettini[1,2]*

[1]Department of Chemistry, Texas A&M University, College Station, Texas 77843-2128, USA
[2]Department of Biochemistry and Biophysics, Texas A&M University, College Station, Texas 77843-2128, USA

Received 1 March 2010; Revised 13 May 2010; Accepted 17 May 2010
DOI: 10.1002/pro.430
Published online 2 June 2010 proteinscience.org

Abstract: PII constitutes a family of signal transduction proteins that act as nitrogen sensors in microorganisms and plants. *Mycobacterium tuberculosis* (*Mtb*) has a single homologue of PII whose precise role has as yet not been explored. We have solved the crystal structures of the *Mtb* PII protein in its apo and ATP bound forms to 1.4 and 2.4 Å resolutions, respectively. The protein forms a trimeric assembly in the crystal lattice and folds similarly to the other PII family proteins. The *Mtb* PII:ATP binary complex structure reveals three ATP molecules per trimer, each bound between the base of the T-loop of one subunit and the C-loop of the neighboring subunit. In contrast to the apo structure, at least one subunit of the binary complex structure contains a completely ordered T-loop indicating that ATP binding plays a role in orienting this loop region towards target proteins like the ammonium transporter, AmtB. Arg38 of the T-loop makes direct contact with the γ-phosphate of the ATP molecule replacing the Mg^{2+} position seen in the *Methanococcus jannaschii* GlnK1 structure. The C-loop of a neighboring subunit encloses the other side of the ATP molecule, placing the GlnK specific C-terminal 3_{10} helix in the vicinity. Homology modeling studies with the *E. coli* GlnK:AmtB complex reveal that *Mtb* PII could form a complex similar to the complex in *E. coli*. The structural conservation and operon organization suggests that the *Mtb* PII gene encodes for a GlnK protein and might play a key role in the nitrogen regulatory pathway.

Keywords: nitrogen regulatory protein; PII; GlnK; GlnB; *Mycobacterium tuberculosis*; binary complex; homology model; glutamine synthetase; ammonium transporter; crystal structure

---

Abbreviations: Mtb, Mycobacterium tuberculosis; *M. jannaschii, Methanococcus jannaschii*; *E. coli, Escherichia coli*; *M. smegmatis, Mycobacterium smegmatis*; 2OG, 2-oxoglutarate; GS, glutamine synthetase; glnD, uridylyl transferase; glnE/ATase, adenylyl transferase; AmtB, ammonia/ammonium transporter; AmtR, transcriptional regulator/repressor; GlnR, transcriptional regulator/activator; ATP, adenosine triphosphate; ADP, adenosine diphosphate; BME, β-mercaptoethanol.

Additional Supporting Information may be found in the online version of this article.

The atomic coordinates and structure factors for *Mtb* apo PII (PDB ID: 3BZQ) and ATP bound *Mtb* PII (PDB ID: 3LF0) have been deposited in the Protein Data Bank.

Grant sponsor: Structural Genomics of Drug Targets from *Mycobacterium tuberculosis*; Grant number: PO1AI068135; Grant sponsor: R.J. Wolfe-Welch Foundation Chair in Science; Grant number: 8–0015.

**Correspondence to:* James C. Sacchettini, Department of Biochemistry and Biophysics, Texas A&M University, College Station, Texas 77843-2128, USA. E-mail: sacchett@tamu.edu

Introduction

The PII family of small signal transduction proteins plays a pivotal role as nitrogen sensors in both microorganisms and plants.[1,2] Nitrogen sensing is achieved by regulating the intracellular nitrogen to carbon ratio represented largely by glutamine and 2-oxoglutarate (2OG), respectively. Intracellular nitrogen regulation is carried out by direct and indirect control of glutamine synthetase (GS) activity through the PII proteins. *E. coli* has two homologues of the PII protein, GlnB (also referred to as PII), encoded by the *glnB* gene, and GlnK, encoded by the *glnK* gene. Under nitrogen limiting conditions, *E. coli* GlnB is uridylylated at a conserved Tyr51 residue by a uridylyl transferase (GlnD), and then interacts with adenylyl transferase to directly activate GS through deadenylylation.[3,4] Conversely, under nitrogen rich conditions, *E. coli* GlnB is deuridylylated by GlnD, and then interacts through the adenylyl transferase to deactivate GS by adenylylation. GlnB has also been shown to form a direct complex with GS in its activation/deactivation cycle in Archaeal *Methanosarcina mazei*.[5] In the indirect control system, *E. coli* GlnB interacts with the two component signal transduction system proteins, NtrB and NtrC, to regulate the transcription of the gene *glnA* which encodes for GS.[6,7] When GlnB is deuridylylated it can interact with a histidine kinase, NtrB, which regulates the phosphorylation state of NtrC, controlling the expression of *glnA*. Thus GlnB is indispensible to the pathway of nitrogen control in *E. coli*.

GlnK is another PII homolog that plays an essential role in the nitrogen control systems of several organisms including *E. coli*[8,9]. In all known instances the *glnK* gene lies in an operon immediately adjacent to the *amtB* gene[10] which codes for the integral membrane protein, AmtB, that acts as ammonia/ammonium channel.[11] Under nitrogen rich conditions in *E. coli* the GlnK trimer complexes with the AmtB trimer blocking the influx of ammonium into the cellular cytoplasm.[9,12] Complex formation between the GlnK protein and AmtB is modulated by the presence of effector molecules like ATP, ADP, and 2OG and is also affected by the post-translational modification of the crucial Tyr51 residue present on the functionally important T-loop of the GlnK protein.[12] In the *E. coli* GlnK, the Tyr51 residue is uridylylated by the GlnD enzyme, but in the Gram-positive soil bacteria *Corynebacterium glutamicum* and *Streptomyces coelicolor* GlnD has been shown to act as an adenylyl transferase, adenylylating instead of uridylylating the GlnK protein at this conserved Tyr51 residue.[13–15] Under nitrogen limiting conditions, the GlnK protein is uridylylated/adenylylated at the Tyr51 residue, which prevents its interaction with AmtB allowing an unhindered flow of extracellular ammonium into the cell through AmtB.[16]

The AmtB:GlnK complex is also implicated in the membrane sequestration of enzymes involved in nitrogen fixation, such as the glycohydrolase DraG in *Azospirillum brasilense*.[17,18] A ternary complex of the AmtB:GlnK with the nitrogen stress transcription factor, TnrA, has also been reported in *Bacillus subtilis*.[19] Similarly, in *Corynebacterium glutamicum,* GlnK interacts with transcriptional repressor AmtR,[20] and in *Streptomyces coelicolor* an OmpR type transcriptional activator, GlnR, has been shown to regulate the expression of *glnK*, *amtB*, *glnA* and *glnD*.[21–23] Thus the AmtB:GlnK complex is capable of functioning with other protein partners like DraG and TnrA to achieve nitrogen regulation and therefore the complex formation is tightly regulated by the presence of effector molecules or post-translational modification at Tyr51 on the T-loop. The PII protein can also complex with N-acetylglutamate kinase (NAGK) to regulate arginine biosynthesis, as seen in the *Arabidopsis thaliana*[24] and *Synechococcus elongates*[25] PII-NAGK complex structures.

Mycobacterium tuberculosis (*Mtb*) has a single *PII* homolog, *Rv2919c*.[26] The *PII* gene was found to be essential for survival in primary murine macrophages by transposon site hybridization (TraSH) in H37Rv.[27] Its essentiality, its roles in nitrogen regulation, and its absence in humans makes PII an attractive drug target in *Mtb,* the causative agent of tuberculosis (TB). The *Mtb* PII gene was annotated *glnB* based on its higher sequence homology to *E. coli* GlnB (www.webTB.org). However, it exists in an operon with *glnD-PII-amtB* (*Rv2918c-Rv2919c-Rv2920c*) leading to speculation that it might encode for a GlnK protein on the basis of the operon organization observed in other microorganisms.[2] The apparent ambiguity requires clear structural and biochemical data to confirm its identity. As part of the *Mtb* structural genomics consortium, we have solved the crystal structure of this protein, both in the apo and ATP bound forms, with the aim of understanding its true identity (and hence its role) in *Mtb,* potentially opening avenues for inhibition studies.[28] The crystal structures presented in this report provide important structural and functional insights into the role of *Mtb* PII as GlnK.

Results and Discussion

Structure of the Mtb apo PII protein

The crystal structure of the *Mtb* apo PII protein was solved at 1.4 Å resolution by molecular replacement using the *E. coli* apo GlnK structure (PDB ID: 1GNK) as the search model. The x-ray diffraction data collection and refinement statistics are in Table I. The crystallographic asymmetric unit contains one subunit, however a homotrimer with identical subunits is

Table I. *Crystallographic and Refinement Statistics*

	Mtb apo PII	*Mtb* PII:ATP
PDB ID	3BZQ	3LF0
Data collection		
Space group	R3	$P4_3\ 2_1\ 2$
Wavelength (Å)	0.96	0.98
Temperature (K)	100	100
a (Å)	77.15	69.74
b (Å)	77.15	69.74
c (Å)	51.84	146.68
α (°)	90	90
β (°)	90	90
γ (°)	120	90
Resolution (Å)	1.40 (1.40–1.44)	2.40 (2.40–2.46)
Unique reflections	21338 (1595)	14020 (982)
% completeness	99.10 (100.0)	99.78 (97.92)
R (merge)	0.06 (0.35)	0.07 (0.63)
⟨I/σI⟩	23.94 (7.77)	12.20 (2.02)
Refinement		
R value (%)	20.80	21.57
Free *R* value, random, 5%	22.60	29.21
Molecules per asymmetric unit	1	3
Protein residues	99	312
ATP molecules	0	3
Rmsd bond length (Å)[a]	0.006	0.017
Rmsd bond angle (Å)[a]	1.007	1.862
Rmsd between subunits (Å)	–	0.31, 0.39, 0.45
Residues φ-ψ angles		
Most favored (%)	98.80	96.60
Allowed (%)	1.20	3.40
Generously allowed/Disallowed (%)	0.0	0.0

[a] Deviations from restraint targets.

formed in the crystal lattice [Fig. 1(A)]. Size exclusion chromatography confirmed that the *Mtb* PII protein exists as a trimer in solution (data not shown).

The structural features of the PII family of proteins from different organisms are well conserved in the *Mtb* PII structure (Fig. 1). The r.m.s.d. of a subunit of *Mtb* apo PII with *E. coli* GlnB (PDB ID: 2PII) is 0.78 Å (for 86 Cα atom pairs–excluding residues 36 to 55 and 109 to 112)[29] and the r.m.s.d. with *E. coli* GlnK (PDB ID: 1GNK–subunit A) is 0.70 Å (for 91 Cα atom pairs–excluding residues 26 and 36 to 55).[30] Figure 1(B) shows a subunit of the *Mtb* apo PII protein with the respective secondary features labeled.[30] In each subunit, connecting strands β2 and β3, is a large loop region of 20 residues that extends out from the main body of the molecule, designated the T-loop (Tyr36 to Phe55). The flexible region of this T-loop, encompassing residues Gln39 through Val53, is disordered in the electron density map and is therefore omitted from the final model of the *Mtb* apo PII structure. The rest of the molecule, including the smaller loop (B-loop) connecting helix α2 and strand β4 is fully ordered. The C-terminal residues extend out from the β4 strand to form a C-loop (Asp97 to Leu112) and has a 3_{10} helix embedded within it between Gly108 and Ala111, consistent with other PII like protein structures.[16,24,30–35]

Structure of the ATP bound Mtb PII protein

The *Mtb* PII:ATP binary complex crystals were obtained by co-crystallization. X-ray data was collected to 2.4 Å resolution and the structure was solved by molecular replacement using the *Mtb* apo PII structure (PDB ID: 3BZQ) as the search model (Data collection and refinement statistics are presented in Table I). Unlike the *Mtb* apo PII protein and the ATP bound *E. coli* GlnK, which have a single subunit in the asymmetric unit, the *Mtb* PII:ATP structure contains a trimer in the asymmetric unit with one ATP molecule bound per subunit [Fig. 2(A) and Supporting information Fig. 1). The crystal structure of *Mtb* PII:ATP shows that ATP binds in three symmetrically equivalent positions in the trimer in a pocket formed by the base of the T-loop, B-loop, and β4 strand of one subunit, and part of the β2 strand, β3 strand, and the C-loop of a neighboring subunit [Fig. 2(B)]. In this structure the ribose ring of ATP adopts the C-3′-endo ring pucker with the adenine ring in the anti-orientation consistent with its position in the *E. coli* GlnK:ATP structure[30] (Supporting information Fig. 1).

The trimeric *Mtb* PII:ATP structure is superposed onto the trimeric *Mtb* apo PII with an r.m.s.d. (between 94 x 3 Cα atom pairs) of 0.69 Å. The r.m.s.d. between the three subunits of the *Mtb* PII protein is 0.31 Å between subunits A and B, 0.39 Å

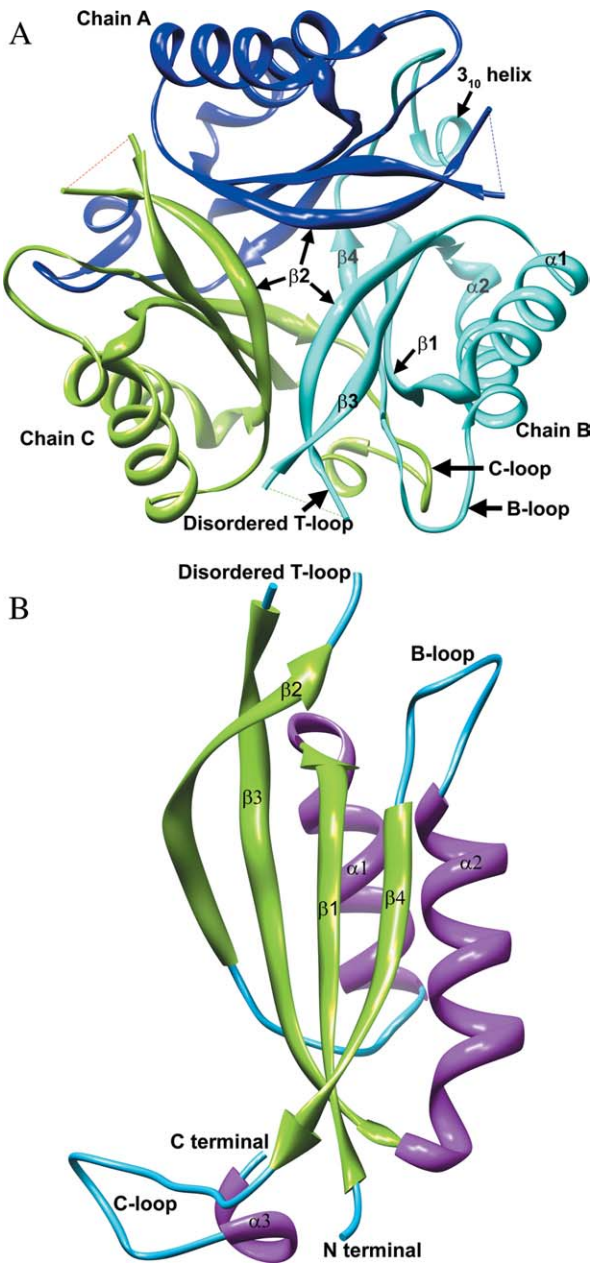

Figure 1. A). A trimer of the *Mtb* apo PII protein viewed down the crystallographic triad showing the three subunits in ribbon representation–A (blue), B (cyan), and C (green). The T-loop region between Gln39 and Val53 is disordered and missing in the *Mtb* apo PII structure. The surface of the trimer assembly carrying the T-loop is designated as the top of the triad and is shown facing up. The β2 strands from the individual subunits form the mouth at the top of the β-barrel, while the β4 strand of each subunit bends inward at the bottom to close the base of the concave β-barrel. The secondary structures are labeled on subunit B (cyan). Molecular graphics images were produced using the UCSF Chimera package from the Resource for Biocomputing, Visualization, and Informatics at the University of California, San Francisco (supported by NIH P41 RR-01081).[56] (B). A single subunit of the *Mtb* apo PII protein is shown in ribbon representation and colored by its secondary structures. The secondary structure features are labeled based on the *E. coli* GlnK structure.[30] The functionally important T-loop is disordered in the *Mtb* apo PII crystal structure.

between subunits B and C, and 0.45 Å between subunits A and C. The differences lie in the positions of the residues in the ATP binding region, whereas the rest of the molecular backbone remains relatively unchanged compared to the *Mtb* apo PII. The disordered T-loop of the apo PII structure is completely ordered in subunit B of the ATP bound *Mtb* PII trimer with the exception of Lys40 and the partially ordered Gln39 [Fig. 2(A) and 3]. However, residues Gln39 to Val53 of subunit A and residues Gln39 to Glu50 of subunit C are disordered and were omitted from the final model of the *Mtb* PII:ATP structure.

The trimer has some distinct structural features that indicate the possible function of the *Mtb* PII protein. In the trimer, the β-sheet from one subunit tilts toward the neighboring subunit at a sheer angle typical of β-barrel structures.[36,37] Three β-sheets, one from each subunit, line the interior of the trimer and enclose a concave β-barrel at the center of the trimer, whereas the α-helices of each subunit lie on the outside of the trimer [Fig. 2(A)]. Glu32 from each β2 strand comes closest to the center at the mouth of the β-barrel, lying symmetrically away from each other at a distance of ~9.1 Å and creating a negatively charged region at the mouth of the β-barrel [Supporting information Fig. 2(A)]. The inner lining of the β-barrel encloses a concave cavity with hydrophobic residues Leu3, Thr5, and Ile7 from the β1 strand, Thr29 and Ile33 from the β2 strand, Val64 from the β3 strand and Trp92 from the β4 strand. In addition, Arg60 and Glu62 from the β3 strands of each subunit insert the polar ends of their side chains into the center of the cavity forming hydrogen bonds to create a charged center, stabilizing the trimer assembly [Supporting information Fig. 2(B)]. Finally, Pro95 residues from each β4 strand are brought into close proximity at the bottom of this barrel at a distance of ~4.0 Å [Supporting information Fig. 2(C)].

An important feature that becomes apparent in the trimeric state is how part of the long C-loop of one subunit lies parallel to the β4 strand of the neighboring subunit making several interactions. For instance, there are hydrogen bonding backbone interactions between Thr98 (C-loop of subunit C) and Val93 (β4 strand of subunit B), Val100 (C-loop of subunit C) with Val91 and Trp92 (β4 strand of subunit B), and Val102 (C-loop of subunit C) with Lys90 (β4 strand of subunit B). The extensive inter-subunit hydrogen bonds between the C-loop of one subunit and the β4 strand of another could be the defining factor in the trimerization of *Mtb* PII. The C-loop of one subunit also approaches the B-loop and the ATP binding site of the neighboring subunit, which may also preserve the structural integrity of the functional trimer. For example, the backbone carbonyl group of Thr104 (C-loop of subunit C) hydrogen bonds with the guanido group of Arg82 (B-loop of

subunit B) at a 2.8 Å distance (Subunit B of *Mtb* PII with a complete T-loop was used to calculate all inter-atomic distances in the ATP binding pocket). The 3_{10} helix at the end of the C-loop contributes to the ATP binding site of the neighboring subunit and is partly stabilized by the hydrogen bonding of the carbonyl group of Ala111 (C-loop) with the amino side chain of Lys90 (β4 strand) (2.8 Å). The importance of the trimeric architecture is that the secondary structural elements involved in the trimerization also form part of the ATP binding pocket indicating that trimerization is critical for its function.

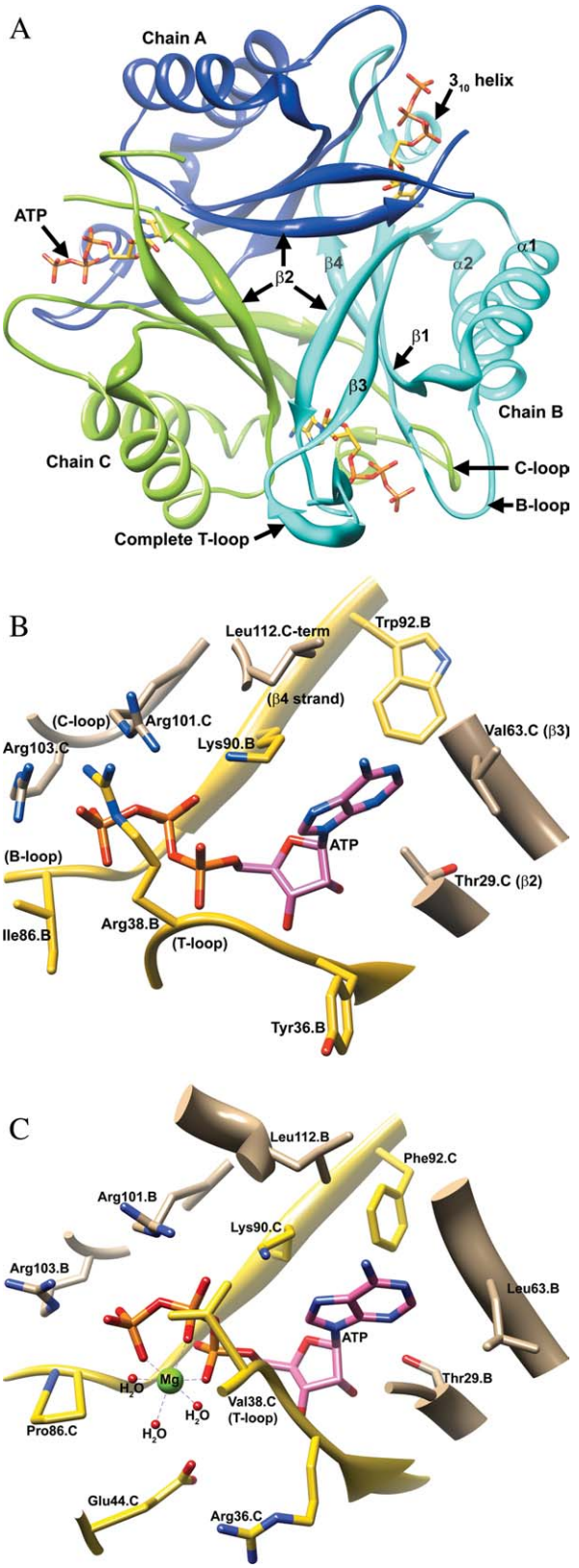

ATP binding site and loop movements–comparison between the apo and ATP bound Mtb PII proteins

There are a number of apo and ATP bound PII crystal structures that have been reported from *E. coli*[16,29–31,34] *Herbaspirillum seropedicae*,[32] *Thermotoga maritima*,[38] *Cyanobacteria Synechococcus* sp. PCC 7942 and *Synechocystis* sp. PCC 6803,[39] *Thermus thermophilus*,[33] *Neisseria meningitidis*,[40] *Methanococcus jannaschii*,[35] *Arabidopsis thaliana*,[24] and *Synechococcus elongatus*.[25] Similar to the discussion of these structures, the protomer ATP interactions in the *Mtb* PII protein can be viewed in reference to three important structural elements, namely the C-loop (3_{10} helix), the B-loop, and the T-loop [Fig. 2(B)]. The C-terminus of the neighboring subunit of *Mtb* PII, aided by a 3_{10} helix, curls back to form part of the ATP binding pocket. The C-terminal residue Leu112 lines a hydrophobic pocket for the adenine ring of ATP, while the terminal carboxylic oxygen atom of Leu112 hydrogen bonds with Arg101 at a distance of 2.8 Å, which in turn hydrogen bonds with the bridge oxygen between the β- and γ-phosphates of ATP (2.9 Å). The 3_{10} helix must

Figure 2. A). A trimer of the *Mtb* PII:ATP binary complex structure is shown viewing down the crystallographic triad. The orientation and color scheme for the trimer assembly is consistent with Figure 1A. Subunit A (blue), B (cyan), and C (green) are represented as ribbons, whereas the bound ATP molecules are shown in yellow stick representation. A complete T-loop is visible in subunit B. (B) The active site of the *Mtb* PII protein bound with ATP (pink). Residues contributed by the neighboring subunit are shown in tan. Residues from the main-chain (Subunit B) are shown in yellow. Conserved residues Gly87.B (B-loop), Gly89.B (B-loop), Lys90.B (β4 strand), and Arg103.C (C-loop) hydrogen bond with the polar phosphate groups of ATP. Residues contributing to adenine binding include Ile7.B (β1 strand), Trp92.B (β4 strand), Leu26.C, Gly27.C, Met28.C, and Thr29.C (in the loop connecting the α1 helix and β2 strand), Val64.C (β3 strand), and Leu112.C (C-loop). (Not all the residues in the ATP binding pocket have been displayed in the interest of clarity). (C) A side by side comparison of the ATP binding pocket of *Mtb* PII:ATP and the *M. jannaschii* GlnK1:ATP(Mg^{2+}):2OG ternary complex structure (PDB ID: 2J9E) is presented.[35] Note that the *Mtb* PII's Arg38 residue is a Val38 in *M. jannaschii* GlnK1. The side chain of Arg38 of *Mtb* PII occupies the Mg^{2+} position of *M. jannaschii* GlnK1.

play a role in the binding of the ATP because it brings Leu112 into proximity with ATP. Furthermore, in the *Mtb* apo PII structure, the Cα atom of Leu112 moves away from the ATP binding site by 1.6 Å and loses its hydrogen bonding interaction with Arg101 although the 3_{10} helix is conserved in the apo structure.

The B-loop carries the conserved mononucleotide binding motif 'Gly(84)-X-X-Gly(87)-X-Gly(89)-Lys(90)' and thus acts as the primary binding site for ATP.[41] Compared to the *Mtb* apo PII structure, the B-loop in *Mtb* PII:ATP moves away from the ATP binding region, making space for the ATP to bind. The Cα atom of Lys85 at the tip of the B-loop moves away by 1.5 Å. The backbone nitrogen atom of Gly89 hydrogen bonds with the oxygen atom of the β-phosphate at a 2.9 Å distance. While the Cα atom of ATP bound and unbound Lys90 are in identical positions, the side chain moves in the ATP bound structure so that the N-Z atom of Lys90 is 5.3 Å away from its position in the apo structure and hydrogen bonds with the β-phosphate of ATP 2.5 Å away.

Arg38 extends out from the base of the T-loop and hydrogen bonds with the oxygen atom of the γ-phosphate at a 3.0 Å distance [Fig. 2(B) and 3]. The binding of ATP is involved in stabilizing the side chain conformation of Arg38, and therefore should partly stabilize the T-loop conformation. In the *Mtb* apo PII structure, the side chain of Arg38 is disordered (along with the T-loop) and is represented as alanine, which could result from a lack of stabilizing interactions in the absence of ATP [Fig. 3]. Indeed, the Cα atom of Arg38 in the *Mtb* apo PII moves away from the active site by 8.3 Å compared to the ATP bound structure, opening this cavity to solvent. This effectively changes the flexibility of the T-loop conformation in *Mtb* apo PII. Comparing the apo and ATP bound structures of the *Mtb* PII protein, it seems apparent that Arg38's interaction with the γ-phosphate is the reason the base of the T-loop moves back into the active site [Fig. 3]. Interestingly, in contrast to the *Mtb* PII and *E. coli* GlnK/B structures, the crystal structure of the *M. jannaschii* GlnK1 shows a Mg^{2+} ion bound next to ATP which coordinates with all three phosphate oxygen atoms[35] [Fig. 2(B,C) for a comparison of the *Mtb* PII and *M. jannaschii* GlnK1 ATP binding sites]. Yildiz *et al.*[35] have argued that Mg^{2+} and ATP are necessary to change the T-loop conformation in the *M. janaschii* GlnK1 protein allowing the creation of the 2OG binding site. In the *Mtb* PII:ATP protein, Arg38 of the T-loop occupies the Mg^{2+} binding site [Fig. 2(B)] to form a direct hydrogen bond with the γ-phosphate oxygen atom of the ATP (3.0 Å). Arg38 of *Mtb* PII is a Val38 in *M. jannaschii* GlnK1 suggesting that a Mg^{2+} is critical for *M. jannaschii* as it is to many other ATP binding proteins. Binding of the Mg^{2+} ion

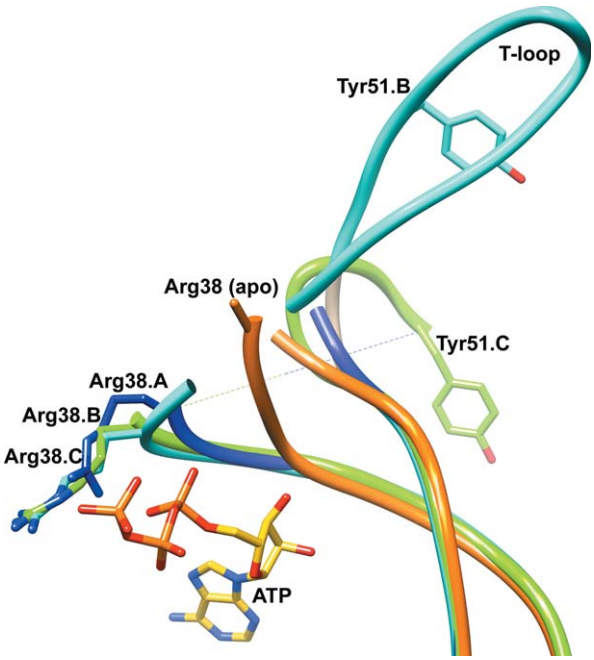

Figure 3. Overlay of the T-loop regions of subunits A (blue), B (cyan), C (green) of the *Mtb* PII:ATP and *Mtb* apo PII (purple) structures, shown in a worm representation. The bound ATP molecule is shown in yellow stick representation. The relative positions of the Tyr51 residues on the T-loop of subunit B (cyan) and subunit C (green) of *Mtb* PII highlight the different orientations of the T-loop in both subunits. Arg38 of the *Mtb* apo PII protein (orange) is modeled as an Ala. Upon binding ATP, Arg38 of all three subunits of the *Mtb* PII:ATP structure (blue, cyan, and green) are stabilized and move relative to their position in the *Mtb* apo PII structure.

pushes the base of T-loop away from the ATP phosphates in *M. jannaschii* GlnK1, whereas in the *Mtb* PII:ATP structure the base of the T-loop approaches ATP (the main chain amide group of Arg38 hydrogen bonds with the ATP α-phosphate at a 3.1 Å distance). The same amide group of Val38 in *M. jannaschii* GlnK1 is 4.7 Å away from the ATP α-phosphate,[35] therefore, it may be that a Mg^{2+} ion is not required by *Mtb* PII for ATP or 2OG binding. In fact, recent *in vitro* studies have shown that the *Mtb* PII binds to both ATP (K_d = 1.93 μ*M*) and 2OG, in the absence of Mg^{2+}.[42] Our attempts to crystallize *Mtb* GlnK in the presence of Mg^{2+} ions were unsuccessful.

While Arg38 forms one part of the enclosure for the phosphates of ATP, Arg103 from the C-loop of the neighboring molecule forms another part of this enclosure forming a hydrogen bond with an oxygen on the γ-phosphate (2.8 Å). Similarly, the C-loop also contributes Arg101, which further stabilizes the ATP binding site; in subunits A, B, and C Arg101 hydrogen bonds with the bridge oxygen between the β- and γ-phosphates of ATP (at distances of 2.8, 2.9, and 3.2 Å, respectively). While Arg38 moves in

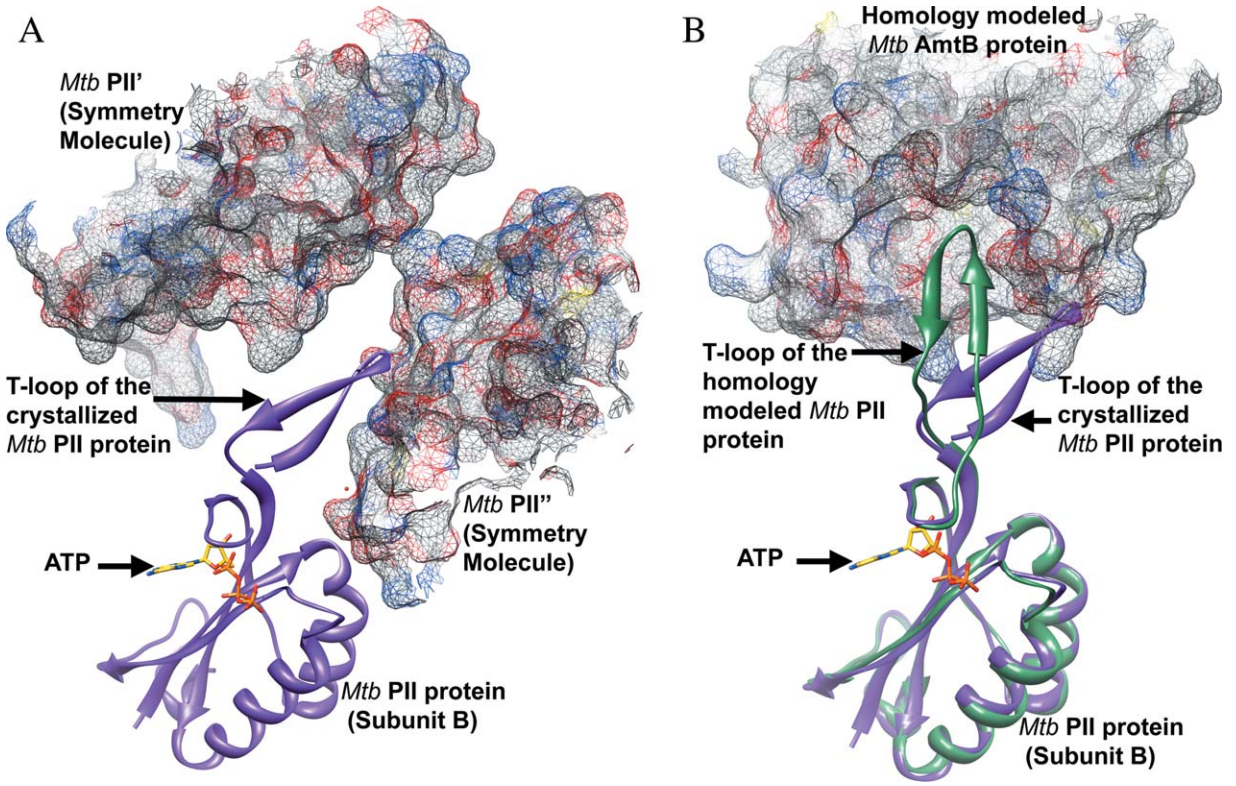

Figure 4. A) Part of the T-loop of subunit B of the *Mtb* PII protein is stabilized by its interaction with the symmetry related molecules *Mtb* PII′ and *Mtb* PII". Subunit B of *Mtb* PII is shown in purple ribbon representation along with the bound ATP in stick representation. The symmetry related molecules *Mtb* PII′ and *Mtb* PII" are shown in mesh representation with 50% transparency.(B) Homology model of *Mtb* AmtB and *Mtb* PII:ATP based on the crystal structure of the *E. coli* GlnK:AmtB complex.[16,34] AmtB is shown in mesh representation with 50% transparency and PII is shown in green ribbon representation. Subunit B of the crystallized *Mtb* PII:ATP structure is superposed on to the homology modeled *Mtb* PII structure and shown in purple ribbon representation along with the bound ATP in stick representation. The superposition highlights the ~45° movement required by the T-loop of the crystallized *Mtb* PII protein to interact with the T-loop binding site of the *Mtb* AmtB protein.

closer to the active site upon ATP binding, Tyr36 moves away (the Cα atom of Tyr36 moves by 2.9 Å) compared to its original position in the *Mtb* apo PII structure. In the ATP bound structure, the backbone nitrogen atom of the Tyr36 forms a hydrogen bond with the 3′ hydroxyl group of ATP (3.2 Å). Therefore, in the ATP bound PII structure, the Tyr36 orients its side chain more closely to the side chain of Phe55 (3.5 Å). As Tyr36 is the first residue and Phe55 is the last residue of the functionally important T-loop, ATP binding can be said to partly influence the orientation of the T-loop itself. Taken together, the binding of ATP along with the positions of Tyr36, Arg38, and Phe55 might contribute to the stability of at least the base of the T-loop of *Mtb* PII and point it in the right orientation to form a complex with PII's target proteins, such as AmtB or GlnD.

Although the residues at the base of the T-loop, including Arg38, are fully ordered in all subunits of *Mtb* PII:ATP (Arg38 is disordered in the apo structure), only subunit B contained the fully ordered T-loop. Upon analyzing the crystal packing effect from the residues of symmetry related molecules on the stability and the conformation of the visible T-loop of subunit B in the *Mtb* PII:ATP structure, we observed that part of the T-loop of subunit B packs inside a groove created by two symmetry related molecules (*Mtb* PII′ and PII″) [Fig. 4(A)]. Tyr51 of the T-loop makes hydrophobic interactions with Val53′ (3.8 Å) of the T-loop from the symmetry related molecule, Tyr46 makes hydrophobic interactions with Ser52′ (3.7 Å), and Glu50 makes a hydrogen bond interaction with Thr98″ (2.5 Å). The backbone amide group of Arg47 hydrogen bonds with the carboxylic acid group of Asp71″ (3.0 Å), and the Cα atom of Arg47 makes a van der Waal's interaction with the side chain of Val70″ (3.8 Å). Overlaying subunit B on subunit A reveals that the T-loop of subunit A is exposed to solvent without any stabilizing interactions, and overlaying subunit B on subunit C of *Mtb* PII revealed clashes of the T-loop with the T-loop from a neighboring symmetry molecule, requiring drastic changes in the T-loop conformation of subunit C to avoid these clashes. Because of this the T-loops in subunits A and C of the ATP bound *Mtb* PII were only partially ordered. It is clear from

the positions of the residues leading up to the missing section of the T-loop in subunit C that the loop has a very different conformation compared to subunits A and B (Fig. 3). Collectively, the interactions of the T-loop of subunit B with the symmetry molecules help stabilize the flexible part of the T-loop, which would otherwise need to be stabilized by forming a complex with a target protein or an effector molecule such as 2OG.[12] Perhaps, the crystal packing effect on the stabilization of the T-loop of subunit B of the *Mtb* PII protein mimics the formation of a complex with a target protein [Fig. 4(A)]. Thus, the T-loop requires some additional stabilizing interactions mediated through the binding of a target protein to *Mtb* PII, in addition to the ATP binding. However, the present conformation of the T-loop is subjective and may adopt different conformations in the presence of a physiological binding partner like AmtB.

Comparison with the E. coli Glnk:AmtB complex

Mtb encodes a probable *amtB* gene (*Rv2920c*), which is next to the *glnB* gene.[26] Comparison between the 428 amino acid *E. coli* AmtB protein and the 477 amino acid *Mtb* AmtB protein shows a 41% sequence identity. All essential residues involved in the interaction of AmtB with the T-loop of PII, specifically Phe107, His168, Phe215, Leu259, Ser263, Val299, Asp313, and His318 of the *E. coli* AmtB, were found to be conserved in *Mtb* AmtB.[34] We constructed a homology model of *Mtb* AmtB and the T-loop section of the *Mtb* PII protein based on the crystal structure of the *E. coli* GlnK:AmtB complex (PDB ID: 2NS1) [Fig. 4(B)] using the SWISS-MODEL program.[43] Comparing the T-loops of subunit B of the *Mtb* PII protein with the homology modeled *Mtb* PII, we noticed that the region of the T-loop that sticks out from the main body of the PII protein swings away from the T-loop binding pocket of AmtB by ~45°. The position of the T-loop observed in the crystal structure of *Mtb* PII:ATP could be due to crystal packing effects (*vide ante*). Thus, in order to bind *Mtb* AmtB, the T-loop would have to swing by ~45° with a maximum movement of ~11.0 Å (observed for the Cα atom of Arg47) to bring the T-loop inside the groove of AmtB [Fig. 4(B)]. However, the base of the T-loop that forms and interacts with the ATP binding site does not move. This suggests that ATP binding stabilizes the base of the T-loop (residues 36–39), but that the rest of the T-loop must be stabilized by a target protein. Given that PII proteins can bind a multitude of target proteins (particularly, AmtB, and GlnD of the same operon[13]), it is logical to think that the T-loop exists in different conformations depending on the target protein it complexes with. For example, in the *Arabidopsis thaliana* PII:NAGK complex structure, the T-loop adopts a very different conformation compared to the *E. coli* PII:AmtB complex structure.[44] The crystal structure of PII:GlnD has not been solved for any organism to date despite strong biochemical evidence for this protein-protein complex formation.[45] Obviously other parameters (like 2OG binding) would influence the conformational changes of the T-loop.

Looking into the T-loop binding pocket of the *Mtb* AmtB homology model, there are few differences when compared with the *E. coli* AmtB structure. The *Mtb* PII protein's Tyr51 terminal hydroxyl group makes favorable hydrogen bonding interactions with the backbone amide of Phe224 of *Mtb* AmtB (2.6 Å). The phenyl ring of Tyr51 makes additional hydrophobic contacts with the side chain of Leu223 (3.3 Å), which does not exist in *E. coli* AmtB, where it is an Ala192. However some hydrogen bonding interactions observed in *E. coli* are missing in *Mtb*, such as the interaction of the backbone carbonyl of Arg47 with Arg253 of *E. coli* AmtB, in *Mtb* it is an Asp284 and is 5.9 Å away. There is also a 36 residue insertion at the C-terminus of the *Mtb* AmtB that hangs on the cytoplasmic side of the membrane that was not included in the homology model, but will be involved in some form of interaction with the PII trimer. Thus the *Mtb* PII protein would be expected to interact and form a complex with the *Mtb* AmtB.

Is the Mtb PII protein a GlnB or GlnK?

The gene encoding *Mtb* PII has been annotated *glnB* in the Tuberculosis Structural Genomics Consortium (TBSGC). Comparing the sequences of other PII proteins from across different species, the *Mtb* PII protein shows a 2 to 7% greater sequence identity with known GlnBs than with their respective GlnKs. (See Table II for comparison of percentage sequence identities with PII proteins from other organisms.) Thus, on the basis of sequence identity alone it could be termed *Mtb* GlnB. However, while the *glnB* gene in most organisms is found in an operon with the *glnA* gene encoding glutamine synthetase, the *glnK* gene in most organisms is linked to an *amtB* gene forming an *amtB-glnK* or *glnK-amtB* operon (and may also contain a third gene, *glnD*). *C. glutamicum* and *S. coelicolor* are two other actinobacteria where the nitrogen regulation pathway has been studied in detail.[46,47] Like *Mtb* they too encode a single homolog of the *PII* gene that lies between the *amtB* and *glnD* genes and the gene product has been annotated as GlnK in both microorganisms based on operon organization. As *Mtb* follows the same operon organization as *C. glutamicum* and *S. coelicolor* it is logical that the gene would also translate into a GlnK protein. Furthermore, it has been suggested that to be annonated *glnB*, the protein product of these genes should consist of a conserved Lys3 and an Asp5 or Glu5.[2] Whereas the *E. coli* GlnB observes this rule, the *Mtb* PII protein has a Leu3 and Thr5, both consistent with *E. coli* GlnK. The

Table II. *Percentage Identity of the Mtb PII Protein with GlnB and GlnK of Other organisms*

	GlnB (% identity with *Mtb* PII protein)	GlnK (% identity with *Mtb* PII protein)
α Proteobacteria		
Azospirillum brasilense	60	56
Rhodospirillum rubrum	57	60
Azorhizobium caulinodans	59	57
β Proteobacteria		
Herbaspirillum seropedicae	64	61
γ Proteobacteria		
Escherichia coli	61	54
Klebsiella pneumoniae	61	54
Firmibacteria		
Bacillus subtilis	–	34
Actinobacteria		
Corynebacterium glutamicum	–	68
Streptomyces coelicolor	–	68
Archaebacteria		
Methanococcus jannaschii	–	55
Cyanobacteria		
Synechococcus	61	–
Plants		
Arabidopsis thaliana	46	–

– a GlnK or GlnB gene does not exist or has not yet been identified.

Lys3 and Asp5/Glu5 residues among GlnB proteins and the Leu3 and Thr5 residues among GlnK proteins are fairly conserved across species, suggesting that the *Mtb PII* gene is in fact *glnK*.[2]

The *Mtb* PII protein projects the Leu3 and Thr5 residues from each subunit into the central cavity of the β-barrel formed by the trimer, while *E. coli* GlnB has Lys3 and Asp5 residues in these positions. The significance of these hydrophilic versus hydrophobic residues at the center of the β-barrel in relation to the function of GlnB and GlnK is unknown and calls for further investigation. Apart from operon organization and sequence specific characterization, the crystal structure of the *Mtb* PII protein gives a clear indication of the nomenclature of the protein. The presence of a 3_{10} helix at the C-terminus of the *Mtb* PII protein is consistent with other known GlnK structures, while in GlnB this region is a loop that is positioned away from the ATP binding pocket. It has been proposed earlier that GlnK structures may differ from GlnB due to the presence of a 3_{10} helix in the C-loop.[30,39,48] For these reasons we suggest that the gene for the PII protein in *Mtb* is *glnK*.

In summary, the operon organization of *Mtb PII* gene, the existence of GlnK specific structural features in both the apo and ATP bound *Mtb* PII crystal structures, and the homology model of the *Mtb* PII:AmtB complex, suggest that the PII homolog of *Mtb* may play a key role as GlnK in the nitrogen regulatory pathway.

Materials and Methods

A 339 bp DNA fragment containing the *PII* gene (*Rv2919c*) was amplified by PCR with *Mtb* H37Rv genomic DNA as a template, using the following oligonucleotide primers:

5′-GGG AAT TCC ATA TGA AGC TGA TCA CTG CGA TCG TGA AGC-3′

3′-CCC AAG CTT TCA TAA CGC GTC GTG TCC GCG TTC AC–5′.

The amplified DNA fragment was digested with *Nde*I and *Hind*III restriction enzymes and subcloned into the corresponding restriction sites in a pET28b vector containing an N-terminal His tag (Novagen). Following sequence confirmation, the plasmid was transformed into *E. coli* BL21(DE3) cells. Cells were induced with 1 m*M* isopropyl-1-thio-β-D-galactopyranoside at A_{600} of 0.8, and grown for 15 h at 25°C. The cells were harvested by centrifugation and lysed by French-press in a buffer containing 20 m*M* tris-HCl, 500 m*M* NaCl, 5 m*M* β-mercaptoethanol (BME), pH 7.5 (buffer A), and a protease inhibitor (Roche Applied Science). The lysate was spun down and the supernatant loaded onto a nickel HiTrap column (GE healthcare). The 12.32 kDa *Mtb* PII protein was eluted with a 100 mL linear gradient of 10 to 500 m*M* imidazole in buffer A. The peak fractions were collected and dialyzed in the presence of 20 m*M* tris-HCl (pH 7.5), 50 m*M* NaCl, 5% glycerol, and 5 m*M* BME and concentrated to 15 mg/mL using an amicon filter (Amicon) as measured by the Bradford protein assay (Bio-Rad).

Crystallization

Initial crystallization conditions were obtained at 289 K in 96-well plates by sitting-drop vapor diffusion. Crystals of the *Mtb* apo PII were obtained by mixing equal volumes of 15 mg/mL protein with a crystallization solution from Crystal Screen™ (Hampton Research) containing 0.1 *M* sodium cacodylate pH 6.5 and 1.4 *M* sodium acetate as precipitant. The *Mtb* PII:ATP binary complex was prepared by mixing the purified 15 mg/mL protein solution with ATP (Sigma) at a final concentration of 5 m*M* and incubating on ice for 30 min. Crystals of *Mtb* PII:ATP were obtained in condition containing 0.1 *M* imidazole pH 6.0 and 1.0 *M* sodium acetate, also from Crystal Screen™.

Data collection, structure determination, and refinement

X-ray diffraction data for *Mtb* PII and *Mtb* PII:ATP crystals were collected on APS beamline 19-ID and 23-ID, respectively. For data collection, a single crystal was cryoprotected by brief soaking in *N*-paratone and then flash-frozen in a liquid N_2 stream (100 K). The HKL-2000 suite[49] of programs was used for integration and scaling of the PII and PII:ATP

complex structures. Crystals of the *Mtb* apo PII protein belong to the space group R3 with unit cell parameters $a = b = 77.15$ Å, $c = 51.84$ Å with one molecule per asymmetric unit and an estimated solvent content of 48.46%. Crystals of the *Mtb* PII:ATP belong to the space group $P4_32_12$ with unit cell parameters $a = b = 69.74$ Å, $c = 146.68$ Å with three molecules per asymmetric unit and an estimated solvent content of 48.1%. Data collection details are summarized in Table I.

The structure of *Mtb* apo PII was solved by molecular replacement using Phaser.[50] The truncated *E. coli* PII structure (PDB ID: 1GNK) lacking the T-loop residues 38–54, was used as search model to solve the *Mtb* apo PII crystal structure.[30] The *Mtb* apo PII structure was used to solve the three positions of *Mtb* PII:ATP structure. After rigid body and restrained refinement using CCP4–REFMAC5[51,52] the model building was carried out in COOT[53] and XTALVIEW[54] for both the structures, solvent molecules were subsequently added. Bias-minimized electron density maps were obtained using the Shake&wARP (SNW) protocol.[55] Each subunit of the *Mtb* PII:ATP structure contained one molecule of ATP with clear electron density (Supporting information Fig. 1).[55,57] and were included in the Refmac refinement. The final *R*-factor for the *Mtb* apo PII crystal structure was 20.80% ($R_{free} = 22.60\%$) at 1.4 Å resolution and for the *Mtb* PII:ATP structure it was 21.57% ($R_{free} = 29.21\%$) at 2.4 Å resolution (Table I).

Acknowledgments

We appreciate the support of staff scientists at beamlines, 19-ID and 23-ID of the Advanced Photon Source, Argonne National Laboratory for their help in data collection. We also thank Misty D. Watson for her excellent technical assistance and Tracey Musa for her comments on the manuscript.

References

1. Ninfa AJ, Atkinson MR (2000) PII signal transduction proteins. Trends Microbiol 8:172–9.
2. Arcondeguy T, Jack R, Merrick M (2001) P(II) signal transduction proteins, pivotal players in microbial nitrogen control. Microbiol Mol Biol Rev 65:80–105.
3. Jiang P, Peliska JA, Ninfa AJ (1998) The regulation of *Escherichia coli* glutamine synthetase revisited: role of 2-ketoglutarate in the regulation of glutamine synthetase adenylylation state. Biochemistry 37:12802–10.
4. Engleman EG, Francis SH (1978) Cascade control of *E. coli* glutamine synthetase. II. Metabolite regulation of the enzymes in the cascade. Arch Biochem Biophys 191:602–12.
5. Ehlers C, Weidenbach K, Veit K, Forchhammer K, Schmitz RA (2005) Unique mechanistic features of post-translational regulation of glutamine synthetase activity in *Methanosarcina mazei* strain Go1 in response to nitrogen availability. Mol Microbiol 55: 1841–54.
6. Ninfa AJ, Magasanik B (1986) Covalent modification of the *glnG* product, NR_I, by the *glnL* product, NR_{II}, regulates the transcription of the *glnALG* operon in *Escherichia coli*. Proc Natl Acad Sci U S A 83:5909–13.
7. Zhang Y, Pohlmann EL, Roberts GP (2005) GlnD is essential for NifA activation, NtrB/NtrC-regulated gene expression, and posttranslational regulation of nitrogenase activity in the photosynthetic, nitrogen-fixing bacterium *Rhodospirillum rubrum*. J Bacteriol 187: 1254–65.
8. van Heeswijk WC, Hoving S, Molenaar D, Stegeman B, Kahn D, Westerhoff HV (1996) An alternative PII protein in the regulation of glutamine synthetase in *Escherichia coli*. Mol Microbiol 21:133–46.
9. Javelle A, Merrick M (2005) Complex formation between AmtB and GlnK: an ancestral role in prokaryotic nitrogen control. Biochem Soc Trans 33:170–2.
10. Thomas G, Coutts G, Merrick M (2000) The *glnKamtB* operon. A conserved gene pair in prokaryotes. Trends Genet 16:11–4.
11. Khademi S, O'Connell J, 3rd, Remis J, Robles-Colmenares Y, Miercke LJ, Stroud RM (2004) Mechanism of ammonia transport by Amt/MEP/Rh: structure of AmtB at 1.35 Å. Science 305:1587–94.
12. Durand A, Merrick M (2006) *In vitro* analysis of the *Escherichia coli* AmtB-GlnK complex reveals a stoichiometric interaction and sensitivity to ATP and 2-oxoglutarate. J Biol Chem 281:29558–67.
13. Strosser J, Ludke A, Schaffer S, Kramer R, Burkovski A (2004) Regulation of GlnK activity: modification, membrane sequestration and proteolysis as regulatory principles in the network of nitrogen control in *Corynebacterium glutamicum*. Mol Microbiol 54:132–47.
14. Read R, Pashley CA, Smith D, Parish T (2007) The role of GlnD in ammonia assimilation in *Mycobacterium tuberculosis*. Tuberculosis (Edinb) 87:384–90.
15. Hesketh A, Fink D, Gust B, Rexer HU, Scheel B, Chater K, Wohlleben W, Engels A (2002) The GlnD and GlnK homologues of *Streptomyces coelicolor* A3(2) are functionally dissimilar to their nitrogen regulatory system counterparts from enteric bacteria. Mol Microbiol 46:319–30.
16. Conroy MJ, Durand A, Lupo D, Li XD, Bullough PA, Winkler FK, Merrick M (2007) The crystal structure of the *Escherichia coli* AmtB-GlnK complex reveals how GlnK regulates the ammonia channel. Proc Natl Acad Sci U S A 104:1213–8.
17. Huergo LF, Merrick M, Pedrosa FO, Chubatsu LS, Araujo LM, Souza EM (2007) Ternary complex formation between AmtB, GlnZ and the nitrogenase regulatory enzyme DraG reveals a novel facet of nitrogen regulation in bacteria. Mol Microbiol 66:1523–35.
18. Huergo LF, Chubatsu LS, Souza EM, Pedrosa FO, Steffens MB, Merrick M (2006) Interactions between PII proteins and the nitrogenase regulatory enzymes DraT and DraG in *Azospirillum brasilense*. FEBS Lett 580: 5232–6.
19. Heinrich A, Woyda K, Brauburger K, Meiss G, Detsch C, Stulke J, Forchhammer K (2006) Interaction of the membrane-bound GlnK-AmtB complex with the master regulator of nitrogen metabolism TnrA in *Bacillus subtilis*. J Biol Chem 281:34909–17.
20. Jakoby M, Nolden L, Meier-Wagner J, Kramer R, Burkovski A (2000) AmtR, a global repressor in the nitrogen regulation system of *Corynebacterium glutamicum*. Mol Microbiol 37:964–77.
21. Wray LV, Jr., Atkinson MR, Fisher SH (1991) Identification and cloning of the *glnR* locus, which is required

for transcription of the *glnA* gene in *Streptomyces coelicolor* A3(2). J Bacteriol 173:7351–60.
22. Fink D, Weissschuh N, Reuther J, Wohlleben W, Engels A (2002) Two transcriptional regulators GlnR and GlnRII are involved in regulation of nitrogen metabolism in *Streptomyces coelicolor* A3(2). Mol Microbiol 46:331–47.
23. Tiffert Y, Supra P, Wurm R, Wohlleben W, Wagner R, Reuther J (2008) The *Streptomyces coelicolor* GlnR regulon: identification of new GlnR targets and evidence for a central role of GlnR in nitrogen metabolism in actinomycetes. Mol Microbiol 67:861–80.
24. Mizuno Y, Moorhead GB, Ng KK (2007) Structural basis for the regulation of N-acetylglutamate kinase by PII in *Arabidopsis thaliana*. J Biol Chem 282: 35733–40.
25. Llacer JL, Contreras A, Forchhammer K, Marco-Marin C, Gil-Ortiz F, Maldonado R, Fita I, Rubio V (2007) The crystal structure of the complex of PII and acetylglutamate kinase reveals how PII controls the storage of nitrogen as arginine. Proc Natl Acad Sci U S A 104: 17644–9.
26. Cole ST, Brosch R, Parkhill J, Garnier T, Churcher C, Harris D, Gordon SV, Eiglmeier K, Gas S, Barry CE 3rd, Tekaia F, Badcock K, Basham D, Brown D, Chillingworth T, Connor R, Davies R, Devlin K, Feltwell T, Gentles S, Hamlin N, Holroyd S, Hornsby T, Jagels K, Krogh A, McLean J, Moule S, Murphy L, Oliver K, Osborne J, Quail MA, Rajandream MA, Rogers J, Rutter S, Seeger K, Skelton J, Squares R, Squares S, Sulston JE, Taylor K, Whitehead S, Barrell BG (1998) Deciphering the biology of *Mycobacterium tuberculosis* from the complete genome sequence. Nature 393: 537–44.
27. Rengarajan J, Bloom BR, Rubin EJ (2005) Genome-wide requirements for *Mycobacterium tuberculosis* adaptation and survival in macrophages. Proc Natl Acad Sci U S A 102:8327–32.
28. Goulding CW, Apostol M, Anderson DH, Gill HS, Smith CV, Kuo MR, Yang JK, Waldo GS, Suh SW, Chauhan R, Kale A, Bachhawat N, Mande SC, Johnston JM, Lott JS, Baker EN, Arcus VL, Leys D, McLean KJ, Munro AW, Berendzen J, Sharma V, Park MS, Eisenberg D, Sacchettini J, Alber T, Rupp B, Jacobs W Jr., Terwilliger TC (2002) The TB structural genomics consortium: providing a structural foundation for drug discovery. Curr Drug Targets Infect Disord 2: 121–41.
29. Carr PD, Cheah E, Suffolk PM, Vasudevan SG, Dixon NE, Ollis DL (1996) X-ray structure of the signal transduction protein from *Escherichia coli* at 1.9 Å. Acta Crystallogr D Biol Crystallogr 52:93–104.
30. Xu Y, Cheah E, Carr PD, van Heeswijk WC, Westerhoff HV, Vasudevan SG, Ollis DL (1998) GlnK, a PII-homologue: structure reveals ATP binding site and indicates how the T-loops may be involved in molecular recognition. J Mol Biol 282:149–65.
31. Cheah E, Carr PD, Suffolk PM, Vasudevan SG, Dixon NE, Ollis DL (1994) Structure of the *Escherichia coli* signal transducing protein PII. Structure 2:981–90.
32. Machado Benelli E, Buck M, Polikarpov I, Maltempi de Souza E, Cruz LM, Pedrosa FO (2002) *Herbaspirillum seropedicae* signal transduction protein PII is structurally similar to the enteric GlnK. Eur J Biochem 269: 3296–303.
33. Sakai H, Wang H, Takemoto-Hori C, Kaminishi T, Yamaguchi H, Kamewari Y, Terada T, Kuramitsu S, Shirouzu M, Yokoyama S (2005) Crystal structures of the signal transducing protein GlnK from *Thermus thermophilus* HB8. J Struct Biol 149:99–110.
34. Gruswitz F, O'Connell J, 3rd, Stroud RM (2007) Inhibitory complex of the transmembrane ammonia channel, AmtB, and the cytosolic regulatory protein, GlnK, at 1.96 Å. Proc Natl Acad Sci U S A 104:42–7.
35. Yildiz O, Kalthoff C, Raunser S, Kuhlbrandt W (2007) Structure of GlnK1 with bound effectors indicates regulatory mechanism for ammonia uptake. Embo J 26: 589–99.
36. Murzin AG, Lesk AM, Chothia C (1994) Principles determining the structure of beta-sheet barrels in proteins. I. A theoretical analysis. J Mol Biol 236: 1369–81.
37. Murzin AG, Lesk AM, Chothia C (1994) Principles determining the structure of beta-sheet barrels in proteins. II. The observed structures. J Mol Biol 236: 1382–400.
38. Schwarzenbacher R, von Delft F, Abdubek P, Ambing E, Biorac T, Brinen LS, Canaves JM, Cambell J, Chiu HJ, Dai X, Deacon AM, DiDonato M, Elsliger MA, Eshagi S, Floyd R, Godzik A, Grittini C, Grzechnik SK, Hampton E, Jaroszewski L, Karlak C, Klock HE, Koesema E, Kovarik JS, Kreusch A, Kuhn P, Lesley SA, Levin I, McMullan D, McPhillips TM, Miller MD, Morse A, Moy K, Ouyang J, Page R, Quijano K, Robb A, Spraggon G, Stevens RC, van den Bedem H, Velasquez J, Vincent J, Wang X, West B, Wolf G, Xu Q, Hodgson KO, Wooley J, Wilson IA (2004) Crystal structure of a putative PII-like signaling protein (TM0021) from *Thermotoga maritima* at 2.5 Å resolution. Proteins 54:810–3.
39. Xu Y, Carr PD, Clancy P, Garcia-Dominguez M, Forchhammer K, Florencio F, Vasudevan SG, Tandeau de Marsac N, Ollis DL (2003) The structures of the PII proteins from the cyanobacteria *Synechococcus sp.* PCC 7942 and *Synechocystis sp.* PCC 6803. Acta Crystallogr D Biol Crystallogr 59:2183–90.
40. Nichols CE, Sainsbury S, Berrow NS, Alderton D, Saunders NJ, Stammers DK, Owens RJ (2006) Structure of the PII signal transduction protein of *Neisseria meningitidis* at 1.85 Å resolution. Acta Crystallogr Sect F Struct Biol Cryst Commun 62:494–7.
41. Walker JE, Saraste M, Runswick MJ, Gay NJ (1982) Distantly related sequences in the alpha- and beta-subunits of ATP synthase, myosin, kinases and other ATP-requiring enzymes and a common nucleotide binding fold. Embo J 1:945–51.
42. Bandyopadhyay A, Arora A, Jain S, Laskar A, Mandal C, Ivanisenko VA, Fomin ES, Pintus SS, Kolchanov NA, Maiti S, Ramachandran S (2010) Expression and molecular characterization of the *Mycobacterium tuberculosis* PII protein. J Biochem 147:279–89.
43. Schwede T, Kopp J, Guex N, Peitsch MC (2003) SWISS-MODEL: An automated protein homology-modeling server. Nucleic Acids Res 31:3381–5.
44. Mizuno Y, Berenger B, Moorhead GB, Ng KK (2007) Crystal structure of *Arabidopsis* PII reveals novel structural elements unique to plants. Biochemistry 46: 1477–83.
45. Bueno R, Pahel G, Magasanik B (1985) Role of glnB and glnD gene products in regulation of the *glnALG* operon of *Escherichia coli*. J Bacteriol 164:816–22.
46. Burkovski A (2007) Nitrogen control in *Corynebacterium glutamicum*: proteins, mechanisms, signals. J Microbiol Biotechnol 17:187–94.
47. Reuther J, Wohlleben W (2007) Nitrogen metabolism in *Streptomyces coelicolor*: transcriptional and post-

translational regulation. J Mol Microbiol Biotechnol 12: 139–46.
48. Xu Y, Carr PD, Huber T, Vasudevan SG, Ollis DL (2001) The structure of the PII-ATP complex. Eur J Biochem 268:2028–37.
49. Otwinowski Z, Minor W (1997) Processing of X-ray diffraction data collected in oscillation mode. Methods Enzymol 276:307–26.
50. McCoy AJ (2007) Solving structures of protein complexes by molecular replacement with Phaser. Acta Crystallogr D Biol Crystallogr 63:32–41.
51. Vagin AA, Steiner RA, Lebedev AA, Potterton L, McNicholas S, Long F, Murshudov GN (2004) REFMAC5 dictionary: organization of prior chemical knowledge and guidelines for its use. Acta Crystallogr D Biol Crystallogr 60:2184–95.
52. Collaborative Computational Project Number 4 (1994) The CCP4 suite: programs for protein crystallography. Acta Crystallogr D Biol Crystallogr 50:760–3.
53. Emsley P, Cowtan K (2004) Coot: model-building tools for molecular graphics. Acta Crystallogr D Biol Crystallogr 60:2126–32.
54. McRee DE (1999) XtalView/Xfit–A versatile program for manipulating atomic coordinates and electron density. J Struct Biol 125:156–65.
55. Reddy V, Swanson SM, Segelke B, Kantardjieff KA, Sacchettini JC, Rupp B (2003) Effective electron-density map improvement and structure validation on a Linux multi-CPU web cluster: The TB Structural Genomics Consortium Bias Removal Web Service. Acta Crystallogr D Biol Crystallogr 59:2200–10.
56. Pettersen EF, Goddard TD, Huang CC, Couch GS, Greenblatt DM, Meng EC, Ferrin TE (2004) UCSF Chimera—a visualization system for exploratory research and analysis. J Comput Chem 25:1605–12.
57. Merritt EA, Murphy ME (1994) Raster3D Version 2.0. A program for photorealistic molecular graphics. Acta Crystallogr D Biol Crystallogr 50:869–73.